J Mater Sci (2009) 44:4522–4530
DOI 10.1007/s10853-009-3660-z

Reinforcement of polysiloxane with superhydrophobic nanosilica

Xu Huang · XianLi Fang · Zhen Lu · Su Chen

Received: 30 April 2009 / Accepted: 1 June 2009 / Published online: 6 July 2009

Abstract We systemically report on a new method for producing reinforced poly(dimethylsiloxane) (PDMS) with superhydrophobic nanosilica. Firstly, we rationally designed to synthesize a series of well-dispersed hydrophobic nanosilica by using hexadecyltrimethoxysilane (HDTMS) as the treatment agent. Fourier transforms infrared (FT-IR) spectrum, thermo-gravimetric analysis (TGA), and contact angle (CA) measurement were used to characterize the grafting degree of HDTMS grafted onto the surface of nanosilica. Subsequently, we employed these modified hydrophobic nanosilica to further reinforce PDMS. The properties of as-prepared modified nanosilica filled PDMS composites were thoroughly investigated by rheological test, scanning electron microscopy (SEM), TGA, and dynamic mechanical analysis (DMA). We have found that these as-prepared superhydrophobic nanosilica exhibit uniform dispersity in the PDMS matrix, and their composites exhibit good mechanical properties and obvious advantage on thermal stability compared with those of the pure silica filled PDMS composites.

Introduction

Reinforcement of polysiloxane with inorganic fillers has not only academic importance in the aspects of polymer–filler interactions and performance-related properties but also in practical applications: the use of the filler as a reinforcement agent usually offers a number of advantages in high modulus, abrasion, and tear resistance [1–5]. Up to now, a variety of elegant efforts have been rapidly proposed for constructing high performance filler reinforced polysiloxane. Schaefer et al. [6] bonded POSS cages to poly (dimethylsiloxane) (PDMS) chains, exhibiting considering improvement on the mechanical properties. Giannelis et al. [7] examined the relationship between nanostructure and properties in silicate/PDMS system. Unfortunately, compared to the substantial empirical attempts, the mechanisms of reinforcement are not fully understood. The design and production of filler-reinforced-polysiloxane have to be mostly depended on a trial and error basis, thereby limiting further development on adequate predictability of performance-related properties and their applications.

For the purpose of more practical applications, most of previous study focused on numerous silica/polysiloxane systems. Paquien et al. [8] investigated the dynamic behavior of fumed silica/PDMS system through controlled silica surface, and set up a relation between the silica grafting ratio, the aggregate size, and the rheological properties. Also sol–gel feeding method is a common method [9, 10]. For example, tetraethoxysilane (TEOS) was first well-dispersed in PDMS matrix, and then decomposed to produce silica with controlled particle size after the hydrolysis and condensation of inorganic precursors, allowing them to disperse in the PDMS matrix in situ. However, this approach gives no mechanical reinforcement comparing with those reinforced with presynthesized silicas. Macosko et al. [11] investigated the dynamic behavior and stress relaxation of silica filled PDMS system as a function of polymer molecular weight, silica concentration, and surface chemistry. Ito et al. [12] studied the effects of surface chemistry of silica particles on the secondary

X. Huang · X. Fang · Z. Lu · S. Chen (✉)
State Key Laboratory of Material-Oriented Chemical Engineering and College of Chemistry and Chemical Engineering, Nanjing University of Technology, No. 5 Xin Mofan Road, Nanjing 210009, People's Republic of China
e-mail: chensu@njut.edu.cn; prcscn@yahoo.com.cn

structure formed by silica particles in styrene–butadiene rubber (SBR). Among them, the degree of silica dispersion and the interactions between the silica and polymer chains are of major importance in the rubber reinforcement. To the best of our knowledge, poor dispersity of silica particles in rubber matrix produced by strong hydrogen bonds between silanol groups on the silica surface can cause a secondary structure (aggregate and agglomerate) of silica particles [12]. The large undispersed agglomerates can produce poor mechanical properties [13, 14] due to failure-initiating flaws in the polymer matrix. Typically, the reinforcement is readily obtained with particle sizes smaller than 100 nm and semi-reinforcement with particle sizes smaller than 1000 nm [1]. Another indication is the interaction between the filler particles and the rubber matrix, which leads to adsorption of polymer chains onto the filler surface or secondary chain entanglement with the shell of the polymer surrounding the particle surface [15]. This interaction may involve the physical properties of the interfacial shell of the polymer surrounding the filler [16], the connecting filaments of the polymer that link aggregates each other [17], the interpenetrating network (IPN)[18] between the filler and polymer matrix. As such, polymer–filler interactions may also contribute to the effective reinforcement.

In order to investigate the mechanisms for silica-filled rubber system, extensive works have been carried out for Payne effect [19–21], bound rubber [22–24], filler flocculation [12, 15, 25], and interfacial effects on viscoelastic behavior [8, 11, 12, 19, 20, 25]. Although numerous efforts have been made on this issue, however, there are no rules that can completely evaluate the special influence of any given filler, or even not all interactions are totally understood. Therefore, understanding this mechanism is critical and instructive to break through the performance ceiling of current silica-filled-polysiloxane composites. By now, there is a general agreement about a three dimensional rubber–filler network contributing to the reinforcement. For filler network, there are two kinds of contact: flexible filler–rubber–filler (FRF) contacts, rigid filler–filler (FF) contacts. The ratio of FRF to FF contacts correlates to surface characteristics, level of filler dispersion, interactions between filler and rubber [12]. As such, it will be beneficial to get better insight on the mechanism of silica-filled rubber reinforcement.

Wettability of surfaces with liquids is a very important character of materials that is governed by both the chemical composition and the geometry of solid surfaces [26]. In our previous study, we developed a convenient and inexpensive approach for formation of a series of superhydrophobic surfaces [27–29]. Here, we first describe a facile strategy toward reinforcing of PDMS with superhydrophobic nanosilica and its potential reinforce mechanism. Initially, we successfully fabricate superhydrophobic nanosilica with contact angle $>150°$ by using hexadecyltrimethoxysilane (HDTMS) grafting onto the surface of nanosilica. And then, we employed contact angle (CA) measurement and thermo-gravimetric analysis (TGA) to investigate the grafting degree of HDTMS on the nanosilica surface. The as-prepared nanosilica tethered with long chain hydrophobic alkyl group allows silica to behave well-dispersed and excellent compatibility in the rubber matrix. It is found that the utilization of as-prepared superhydrophobic nanosilica in the PDMS composites can lead dramatic reinforcement by the results of the investigations of rheological properties, tensile properties, TGA, bound rubber, and dynamic mechanical properties.

Experimental

Materials

Poly(dimethylsiloxane) (PDMS, $M_w = 7.0 \times 10^5$, 0.17 mol% vinyl groups) was purchased from Dongjue Silicone Group Co. Ltd (Nanjing) and fumed silica (A380, specific surface area 380 m^2/g) was provided by Shenyang Chemical Co. Ltd (Shenyang). The process aid (hydroxyl-terminated low molecular weight polydimethylsiloxane fluid) and peroxide catalyst 2,5-dimethyl-2,5-di(tert-butylperoxy) hexanes were supplied by Aldrich and used as received. Toluene (China National Medicine Cor. Ltd) and hexadecyltrimethoxysilane (HDTMS) (Sigma-Aldrich) used as surface modifier were used directly from the manufacturer without further purification.

Fabrication of superhydrophobic nanosilica

The surface modification of the silica was achieved according to the following procedure. Fumed silica was firstly dispersed in toluene and exposed under ultrasound till the formation of the transparent solution (about 30 min). After that, the mixture was heated to 80 °C and added HDTMS in drops under magnetic stirring. Subsequently the mixture was refluxed at 110 °C for 6 h. Finally, the product was suffered repeated disperse-wash-centrifuge cycles in toluene and was dried under vacuum overnight at 80 °C. We prepared the modified nanosilica with different HDTMS-to-silica weight ratios, 1:3, 2:3, 3:3, and 5:3, respectively (denoted as S1, S2, S3, and S4).

Preparation of modified silica/PDMS blends and their vulcanizates

The as-prepared modified silica was incorporated into PDMS by a torque rheometer (XSS-300, Kechuang Machinery, Shanghai) with a chamber capacity of 200 mL

at 50 °C and a fixed rotor speed of 30 rpm. PDMS was added into the mixing chamber and softened without filler. Then half amount of filler was poured into mixing chamber and after 5 min mixing processing, the rest modified silica was added and mixed for another 10 min. To obtain the homogeneous dispersion of filler, the blends were further homogenized by an open two-roll mill at room temperature for 10 min. The vulcanizates were prepared at a curing press for 10 min under 170 °C, and the peroxide catalyst was added into the blends prior to the curing process.

Characterization

The chemical structure of modified nanosilica was analyzed by Fourier transform infrared (FT-IR) spectrum in the range of 400–4000 cm^{-1} using a Nicolet 6700 spectrometer (KBr disk, 64 scans, 4 cm^{-1} resolution). The grafting percentages of modified nanosilica were determined by thermogravimetric analysis (TGA) on a Shimadzu TGA-50 with a heating rate of 10 °C/min from 38 to 700 °C. Water contact angle measurement was implemented using a 5 μL water droplet on the surface measured with a KRüSS DSA100 (KRüSS, Germaemny) contact-angle system at ambient temperature. A field emission electron microscopy (FEEM: HITACHI-S-4800) was employed to observe the fracture surfaces of filled PDMS, obtained from cryogenically fracturing in liquid nitrogen, and subsequently coated with gold thin layer using a SEM coating machine. Bound rubber test was carried out in toluene to dissolve extractable part in the PDMS blends. The extraction took place for 3 days in the Soxhlet apparatus, and the non-extracted part (gel) was dried at 80 °C for 48 h in a vacuum oven to remove the adsorbed solvent. The calculation for the bound rubber (BDR) in the compound is given by as follows,

$$\mathrm{BDR}(\%) = \frac{\text{Amount of rubber in unextracted gel}}{\text{Initial amount of rubber in compound}} \times 100 \quad (1)$$

The vulcanized sheet with a thickness of about 2 mm was die-cut to a dumbbell-shaped specimen and tested at a crosshead speed of 500 mm/min according to GB/T 528 with an electronic universal testing machine (CMT-5254, Sans Group). Rheological properties was measured by a rotary rheometer in a parallel plate geometry (Aaton Paar Physica MCR301), with a strain amplitude ranging from 0.01 to 1000% at fixed frequency of $\omega = 0.63$ rad/s. Dynamic mechanical analysis (DMA) of the vulcanizates was carried out in NETZSCH DMA 242, in a temperature range between −150 °C and 50 °C, at a constant frequency of 1 Hz, and at a heating rate of 2 °C/min.

Results and discussion

Synthesis of superhydrophobic nanosilica and characterization

The synthesis of superhydrophobic silica involves functionalizing nanosilica with HDTMS as described in Scheme 1. To gain complete encapsulation of silica nanoparticles with HDTMS, the amount of HDTMS used here was excess, ensuring the silanol groups of nanosilica to completely react with the alkoxylsilane groups of HDTMS. The maximum functionality of nanosilica via the reaction between silanol groups and the alkoxylsilane functionalities is favorable to further improve the filler dispersion and its miscibility with the polymer matrix.

In order to investigate chemical structure of modified nanosilica, we use FT-IR to characterize the samples of modified nanosilica, along with the control sample for comparison (as shown in Fig. 1). Figure 1a–d and e present the FT-IR spectra of modified nanosilica with different concentrations of HDTMS in the modified nanosilica and pure nanosilica, respectively. Comparing FT-IR results of modified nanosilica (Fig. 1a–d) with that of pure nanosilica (Fig. 1e), we have found that there are new absorption peaks in the spectra of modified nanosilica occurred at 1460 cm^{-1} (νCH_2), 2925 cm^{-1} (νCH_2), and 2858 cm^{-1}(νC–H), confirming the condensation reaction between methoxy group of HDTMS and hydroxyl groups on the surface of nanosilica. As seen in Fig. 1a–d, we have also found that the intensity of absorption peaks noticed at 1460 cm^{-1} (νCH_2), 2925 cm^{-1} (νCH_2), and 2858 cm^{-1}, respectively, get stronger with increasing concentration of HDTMS in the modified nanosilica as well as the absorption peaks of Si–OH group in the spectra of modified nanosilica turn weaker, correspondingly. The FT-IR results also present that the grafting degree of HDTMS grafting onto the surface of nanosilica is ascended as the increase of HDTMS content in the modified nanosilica.

The grafting percentages of modified nanosilica were determined by TGA measurement under a nitrogen atmosphere. In order to obtain exact results of TGA, all the samples were washed and isolated completely for several

Scheme 1 Schematic formation of superhydrophobic nanosilica

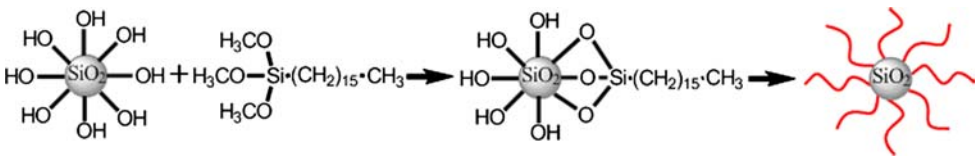

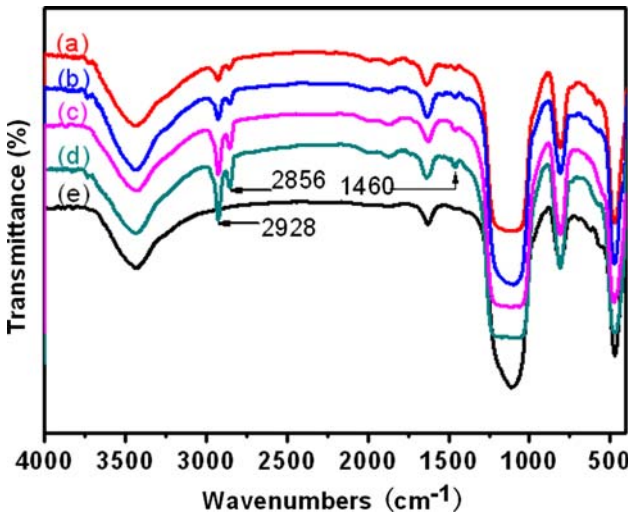

Fig. 1 FT-IR spectra of **a** HDTMS/nanosilica = 1/3 wt%, solvent: toluene, reaction time: 6 h; **b** HDTMS/nanosilica = 2/3 wt%, solvent: toluene, reaction time: 6 h; **c** HDTMS/nanosilica = 3/3 wt%, solvent: toluene, reaction time: 6 h; **d** HDTMS/nanosilica = 5/3 wt%, solvent: toluene, reaction time: 6 h; and **e** pure nanosilica

times, allowing free HDTMS to be completely removed. Figure 2 exhibits the TGA curves of modified nanosilica S1, S2, S3, and S4, respectively. According to following Eq. 2, the individual grafting percentages of S1, S2, S3, and S4 are 1.9, 3.9, 5.9, and 6.1%, respectively, which are increased with the concentration of HDTMS in the modified nanosilica. These TGA results are in good agreement with the FT-IR spectra results, showing that HDTMS have been successfully grafted onto the surface of nanosilica.

$$\text{Percentage of grafting}(\%) = \frac{\text{Organic modifier grafted (g)}}{\text{Silica used (g)}} \times 100\% \quad (2)$$

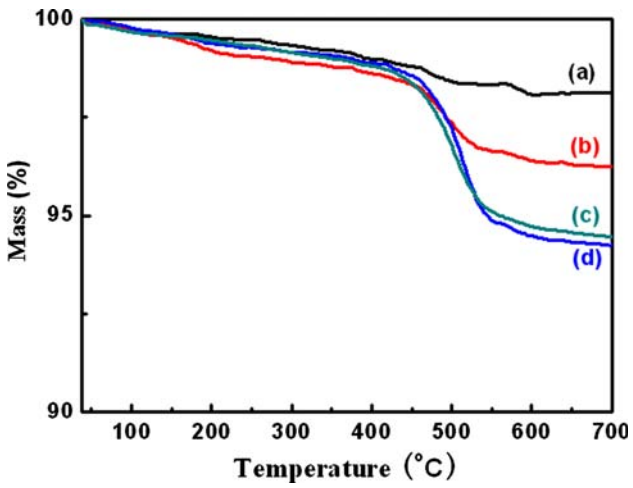

Fig. 2 TGA curves for modified silica at different mass ratios: a = 1:3; b = 2:3; c = 3:3; and d = 5:3 (HDTMS/Silica, wt/wt)

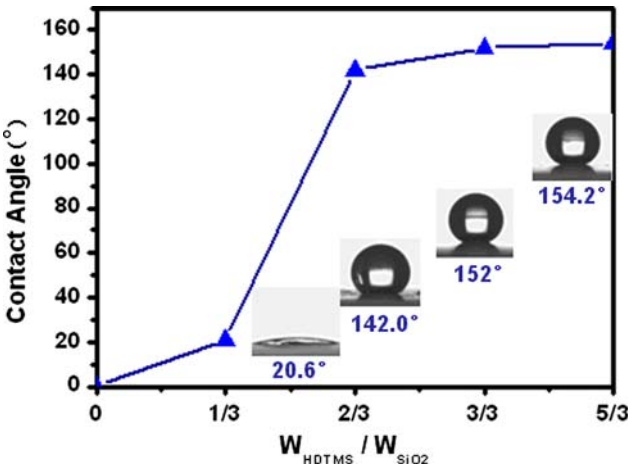

Fig. 3 Water contact angle for modified silica at different mass ratios: 1:3; 2:3; 3:3; and 5:3 (HDTMS/Silica, wt/wt)

To investigate the hydrophobic properties of the modified nanosilica, we measured water contact angles (CAs) of modified nanosilica samples, along with the sample of pure silica, respectively. Figure 3 presents the CA values of modified nanosilica as a function of different weight ratios of HDTMS to nanosilica. As shown in Fig. 3, the CA value of the modified nanosilica is dramatically increased with the elevated concentration of HDTMS in the modified nanosilica. When the weight ratio of HDTMS to nanosilica reaches 3/3 (wt/wt), the CA value of the modified nanosilica is up to 152°, which corresponds with the criteria of the superhydrophobic surface, with a water CA larger than 150°. While continuing to increase the HDTMS content, the CA value of the modified nanosilica varies slightly. This trend effect coincides with the grafting degree of the modified nanosilica as a function of HDTMS content. Namely, it implies that the CA value of the modified nanosilica can correspond with the grafting degree of HDTMS grafting onto the surface of nanosilica in this case.

Rheological properties of silica/PDMS blends

In an effort to understand the influence of the as-prepared superhydrophobic silica on the rheological properties of silica/PDMS blends, we carried out rheological measurements to investigate their roles in determining the corresponding filler–PDMS networks. Figure 4 presents variation of storage modulus versus strain amplitude behavior for S3/PDMS blends with different filler loadings, along with the corresponding control sample of A380/PDMS blends for comparison. As shown in Fig. 4, with increasing filler loadings, the hydrodynamic effect serves as the incorporation of fillers, leading to a strain independent increase in modulus, while Payne effect [21], reflecting the viscoelastic response of the rubbery material to periodic deformation and

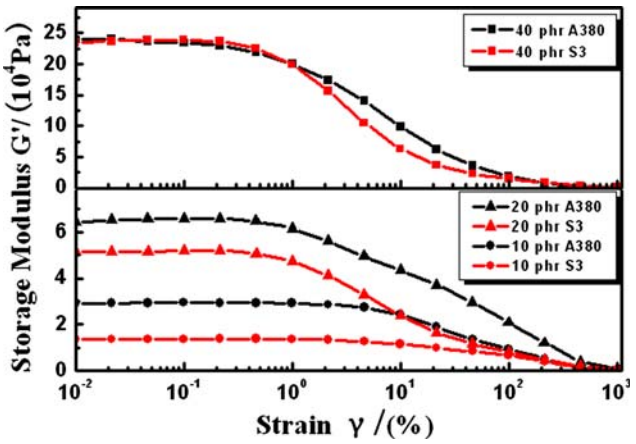

Fig. 4 Variation of storage modulus versus strain amplitude for A380/PDMS and S3/PDMS blends with different filler loadings

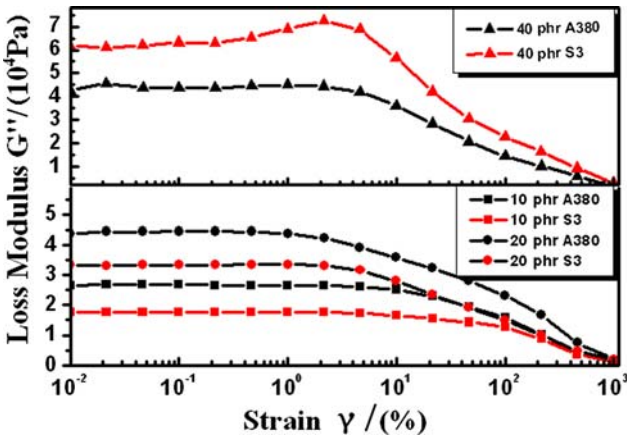

Fig. 5 Variation of loss modulus versus strain amplitude for A380/PDMS and S3/PDMS blends with different filler loadings

the networks' transformation at the low strain amplitudes, is especially remarkable in this case. In contrast with the untreated silica system, the storage modulus of S3/PDMS filled with superhydrophobic silica (filler loading <40 phr) at low filler loadings is significantly lower than those corresponding to the control samples of A380/PDMS. This is mainly due to the good miscibility between the superhydrophobic nanosilica filler and PDMS, and weak filler–filler interactions between these modified fillers. Also, the higher G' of A380/PDMS can be attributed to large amounts of direct filler–filler contacts due to the poor dispersion of silica in PDMS. With the increase in strain, G' decreases accompanying with the breakage of the filler network. It is notable that when silica loading reaches to 40 phr, the values of G' for both S3/PDMS and A380/PDMS system are almost same. We believe that the filler–polymer–filler interactions compensate the modulus loss caused by the weak filler–filler interaction for S3/PDMS blend. For superhydrophobic nanosilica, the long alkyl chain tethered outside nanosilica behaves good compatibility with polymer. And the polymer can be easily absorbed on the surface of silica to form the bound layer. Therefore, this bound layer can further entangle with the PDMS matrix, leading to the subtle changes of network. Similar results were also found in the literature reported by Giannelis [30].

Figure 5 presents variation of loss modulus versus strain amplitude behavior for S3/PDMS blends with different filler loadings, along with the corresponding control sample of A380/PDMS blends for comparison. In contrast with the untreated silica system, the loss modulus of S3/PDMS filled with superhydrophobic silica (silica content <40 wt%) at low filler loadings is much lower than those corresponding to the control samples of A380/PDMS. It is also explained by that the superhydrophobic silica have the good miscibility with PDMS matrix, and weak filler–filler interaction. However, the loss modulus of the S3/PDMS system is much higher than that of A380/PDMS system at the filler loading of 40 phr. Also, a maximum loss modulus could be observed in S3/PDMS blend at the filler loading of 40 phr, indicating the occurrence of strain-induced agglomeration. Based on the literature reported by Macosko et al. [11] typically, there are three types of linkages responsible for this agglomeration: direct bridge, primary entanglement, and secondary entanglement. In the case of superhydrophobic silica filled PDMS system, the direct bridge mainly caused by silica aggregation may be greatly reduced thanks for the slippery surface of superhydrophobic nanosilica. On other hand, the later two linkages are supposed to explain the occurrence of maximum loss modulus noticed in Fig. 5 and the compensation effect of storage modulus in Fig. 4 at the filler loading of 40 phr. Loss factors tan δ of A380/PDMS and S3/PDMS as a function of strain are presented in Fig. 6. At low strains, the

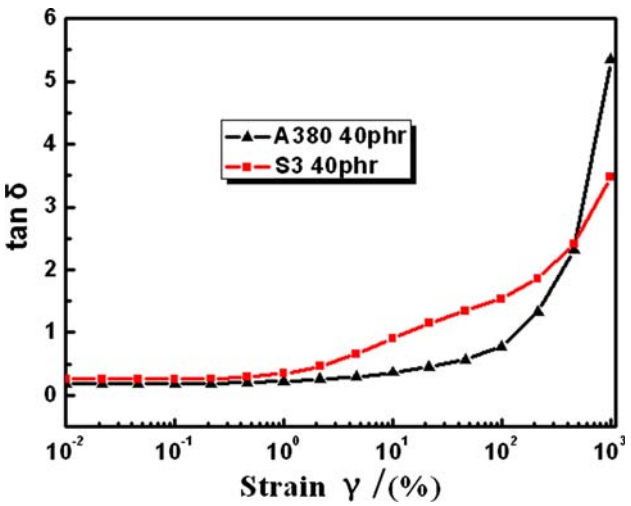

Fig. 6 Curves of tan δ versus strain amplitude for A380/PDMS and S3/PDMS blends at the same filler loading of 40 phr

tan δ of S3/PDMS is larger than that of A380/PDMS, whereas at high strains, this trend completely reverses. This effect is attributed to the different modes of the energy dissipation at low and high strain region. At strain <500%, the filler network of S3/PDMS is well-preserved and the viscous nature of rubber is mainly responsible for the energy dissipation. Compared to S3, the dispersion of A380 in PDMS is poorer, resulting direct FF contact dominating in this system. Thus, in A380/PDMS, the rubber entrapped within the unmodified silica shields from deformation, leading to the reduced deformable rubber fraction. However, by contrast, at strain >500%, due to the viscous characteristic of rubber and the hysteresis effect, tan δ of A380/PDMS is larger than that of S3/PDMS. This phenomenon is likely attributed to the reduction of chemical interfacial interaction in superhydrophobic silica filled PDMS system [31].

Bound rubber measurements and mechanical properties

We evaluate the bound rubber of as-prepared nanosilica filled PDMS in terms of the reported procedure, along with the control sample for comparison [22]. As shown in Table 1, the values of the bound rubber with respect of A380/PDMS, S1/PDMS, S2/PDMS, and S3/PDMS are 60.06, 50.64, 44.39, and 34.79%, respectively. The results indicate that the amount of bound rubber for A380/PDMS is larger than those of the as-prepared nanosilica filled PDMS system. Also, with the elevated contact angle of the modified nanosilica, the amount of bound rubber for the as-prepared nanosilica filled PDMS further decreases correspondingly. In the view of the reported literature [32], the degree of bound rubber is mostly depended on the hydroxyl content of silica since the hydroxyl groups on the surface of silica can serve as forming crosslinked structure in the silica filled rubber system. Obviously, the hydroxyl content of nanosilica after modifying with silane could dramatically reduce, leading to the decrease of the amount of the bound rubber. Based on the traditional viewpoint, the enhanced bound rubber contributes to reinforce silicone rubber. However, we suggest that is not only criteria for reinforcement of rubber. It is necessary to combine the effects on the dispersion and compatibility of silica with the rubber.

Table 1 The effect of fillers with different surface wettability on bound rubber content

Filler	A380	S1	S2	S3
Bound rubber %	60.06%	50.64%	44.39%	34.79%
CA (°)	0°	20.6°	142°	152°

PDMS 100 phr; filler 40 phr; and process aid: 3 phr (for all blends testing for bound rubber)

Table 2 Mechanical properties of HDTMS modified silica filled PDMS

Samples	Tensile strength (MPa)	Elongation at break (%)
PDMS gum	0.35	101.4
A380/PDMS	6.31	320.28
S1/PDMS	5.07	302.7
S2/PDMS	5.62	411.1
S3/PDMS	6.80	460.1

PDMS 100 phr; filler 40 phr; process aid 3 phr; curing agent 1 phr; and curing temperature 170 °C

This viewpoint is likely supported by the mechanical properties of as-prepared nanosilica filled PDMS shown in Table 2. As indicated in Table 2, initially, the tensile strength of S1/PDMS and S2/PDMS is lower than that of A380/PDMS. Perhaps more interestingly, when the modified nanosilica is up to be superhydrophobic nanosilica (S3, CA = 152°), the tensile strength and elongation at break of S3/PDMS is larger than those of A380/PDMS. In this case, the dispersion and compatibility of nanosilica with the rubber is mostly predominant in the reinforcement effect.

Dynamic mechanical properties

The influence of the superhydrophobic nanosilica filled PDMS on the loss modulus G'' and the damping factor tan δ, along with the control sample, is depicted in Figs. 7 and 8. As shown in Fig. 7, the significant rise in the loss modulus over the analyzed temperature range can be observed when we employed different modified hydrophobic nanosilica in the PDMS matrix. Figure 8 presents

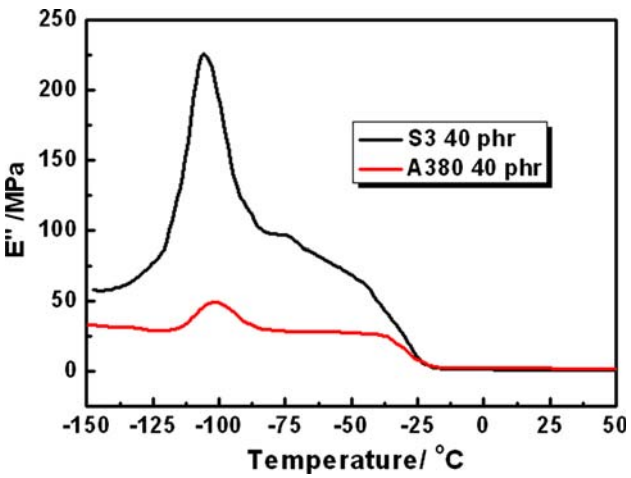

Fig. 7 Curves of loss modulus versus temperature at 1 Hz for cured A380/PDMS, S2/PDMS, and S3/PDMS (PDMS 100 phr; filler 40 phr; process aid 3 phr; curing agent 1 phr; and curing temperature 170 °C)

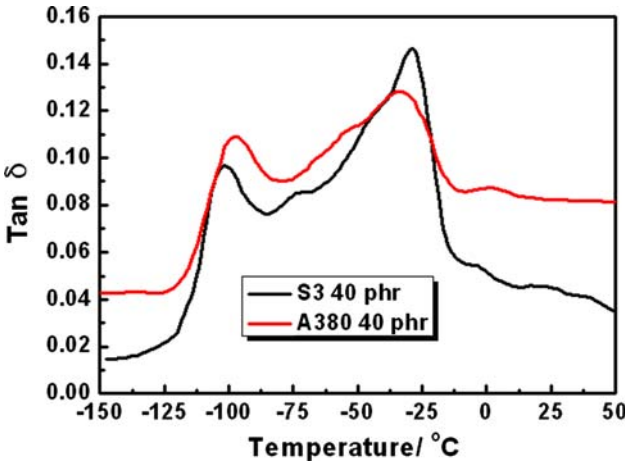

Fig. 8 Curves of tan δ versus temperature at 1 Hz for cured A380/PDMS, S2/PDMS and S3/PDMS (PDMS 100 phr; filler 40 phr; process aid 3 phr; curing agent 1 phr; and curing temperature 170 °C)

the damping factor tan δ over the analyzed temperature with the superhydrophobic nanosilica or unmodified nanosilica filled PDMS, respectively. It is noted that the T_g of S3/PDMS at lower temperature is lower than that of A380/PDMS. However, the T_g of S3/PDMS at higher temperature is much larger than that of A380/PDMS. The shift of main relaxation toward the lower temperature has been mainly attributed to an increase in the molecular motion of the polymer in the vicinity of the filler surface [33].

Morphology and reinforcing mechanism

The fracture morphologies of A380/PDMS and S3/PDMS are shown in Fig. 9. From Fig. 9a, the filler A380 without any modification presents poor dispersion in PDMS matrix, and even significant aggregations occurs in this case. Moreover, the interfacial region between fillers and PDMS matrix is unambiguous and recognizable, allowing a spectrum of flaws to exist in the surrounding of aggregated fillers. However, in the superhydrophobic nanosilica filled PDMS system, well-dispersed modified nanosilica in the PDMS matrix is obviously observed in Fig. 9b. The interfacial region between fillers and PDMS matrix becomes ambiguous, indicating that obviously good miscibility between the filler and PDMS exists when we employed superhydrophobic nanosilica to fill in PDMS matrix. Also, the flaws in S3/PDMS system are dramatically decreased in this circumstance. This effect favors to improve the mechanical properties of reinforced PDMS.

Considering the structure defects are always the inducements of the materials' failure behaviors, we proposed the assumed reinforcement mechanism of filled rubber presented in Fig. 10. For pure silica filled PDMS, the rich silanol groups on the surface of pure silica severs to produce a larger rigid filler–filler (FF) contact via hydrogen bonds, leading the occurrence of silica aggregations and poor dispersion. This enforced FF interaction may result the reduction of flexible filler–rubber–filler (FRF) interactions, allowing the ratio of FRF to FF interactions to further decrease. However, for superhydrophobic nanosilica filled PDMS, the dispersion and miscibility between the filler and PDMS can be remarkably improved after intensifying surface hydrophobicity of nanosilica. Meanwhile, it can efficiently reduce the FF interactions, and enable FRF interaction not to be further decreased. Therefore, the ratio of FRF to FF interaction for S3/PDMS may be larger than that of A380/PDMS. This phenomenon is already confirmed by the SEM results shown in Fig. 9 and the results of rheological properties. We believe the elevated ratio of FRF to FF favors to enhance the reinforced effect of filled rubber.

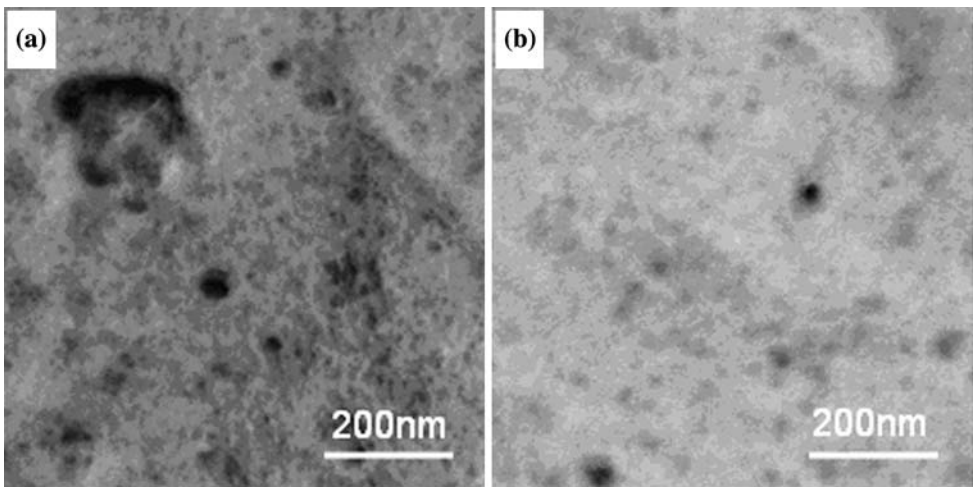

Fig. 9 SEM images of cured PDMS after reinforcement: **a** A380/PDMS; **b** S3/PDMS (PDMS 100 phr; filler 40 phr; process aid 3 phr; curing agent 1 phr; and curing temperature 170 °C. Dark zone represents silica and bright zone is PDMS)

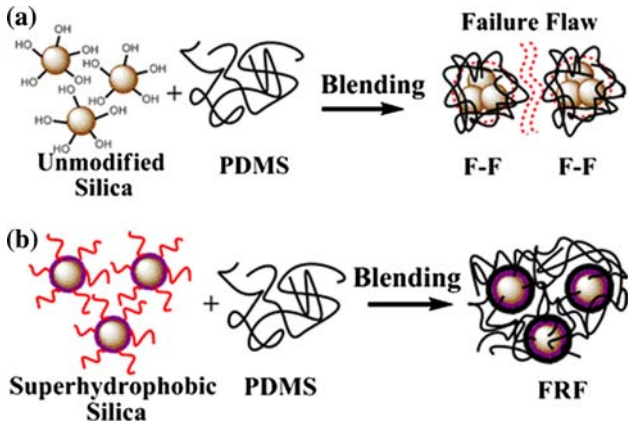

Fig. 10 The assumed reinforcement mechanism for: **a** untreated and **b** superhydrophobic nanosilica filled PDMS system

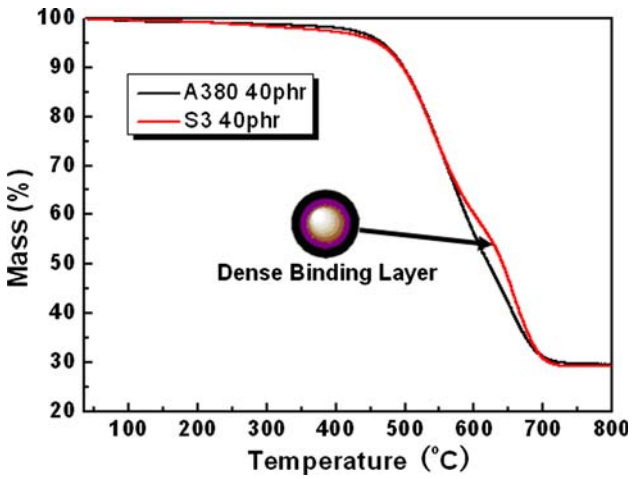

Fig. 11 TGA curves for the A380/PDMS and S3/PDMS vulcanizates (PDMS 100 phr; filler 40 phr; process aid 3 phr; curing agent 1 phr; and curing temperature 170 °C)

TGA measurement

Typical TGA results for A380/PDMS and S3/PDMS are shown in Fig. 11. As shown in Fig. 11, by comparison, there are two degradation steps in S3/PDMS, while only single degradation step exists in A380/PDMS. Also, the thermal stability for these two kinds of samples is almost similar when the temperature is lower than 570 °C. However, with the temperature >570 °C, the thermal stability for S3/PDMS is much better than that of A380/PDMS. We attribute the second degradation step in the range from 570 °C to 700 °C for S3/PDMS is mainly due to the fact that there is a dense binding layer between the modified nanosilica and PDMS matrix. This find is the direct evidence that the as-prepared superhydrophobic nanosilica, compared with unmodified silica, can efficiently reinforce PDMS.

Conclusions

This study has demonstrated a new method for producing reinforced PDMS with superhydrophobic nanosilica. Using HDTMS as the surface treatment agent, we successfully prepared the superhydrophobic nanosilica with contact angle of about 152°. It has been found that the as-prepared superhydrophobic nanosilica present uniform dispersity in the PDMS matrix, and their composites exhibit high performance on tensile strength and elongation at break. Also the S3/PDMS composites shows the obvious advantage on thermal stability compared with those of the pure silica filled PDMS composites. A series of characterizations, such as rheological test, SEM, TGA, and DMA, allow us to get better insight on the reinforcement mechanism of silica filled PDMS. The systematic work to that of this investigation constitutes a promising way to fabricate other robust silica filled rubbers.

Acknowledgements This work was supported by Natural Science Foundations (NSFs) of China (Grant No. 20576053, 20606016), NSF (NASA) of China (Grant No. 10676013), "863" Important National Science and Technology Specific Project (Grant No. 2007AA06A402), and the NSF of the Jiangsu Higher Education Institutions of China (Grant No. 07KJA53009).

References

1. Pérez LD, Giraldo LF, López BL, Hess M (2006) Macromol Symp 245–246:628
2. Okel TA, Waddell WH (1994) Rubber Chem Technol 68:59
3. Cochrane H, Lin CS (1992) Rubber Chem Technol 66:48
4. Lutz MA, Polmanteer KE, Chapman HL (1988) Rubber Chem Technol 58:939
5. Polmanteer KE (1987) Rubber Chem Technol 61:470
6. Pan GR, Center JE, Schaefer DW (2003) J Polym Sci Part B Polym Phys 41:3314
7. Burnside SD, Giannelis EP (2000) J Polym Sci Part B Polym Phys 38:1595
8. Paquien JN, Galy J, Gérard JF, Pouchelon A (2005) Colloids Surf A 260:165
9. Dewimille L, Bresson B, Bokobza L (2005) Polymer 46:4135
10. Yuan QW, Mark JE (1999) Macromol Chem Phys 200:206
11. Aranguren MI, Mora E, DeGroot JV Jr, Macoskoa CW (1992) J Rheol 36(6):1165
12. Suzuki N, Yatsuyanagi F, Ito M, Kaidou H (2002) J Appl Polym Sci 86:1622
13. Crosby AJ, Lee JY (2007) Polym Rev 47:217
14. Coran AY, Ignatz-Hoover F, Smakula PC (1993) Rubber Chem Technol 67:237
15. Léopoldès J, Barrès C, Leblanc JL, Georget P (2004) J Appl Polym Sci 91:577
16. Maier PG, Göritz D (1996) Kautsch Gummi Kunstst 49:18
17. Heinrich G, Klüppel M (2002) Adv Polym Sci 160:1
18. Deng Q, Hahn JR, Stasser J, Preston JD, Burns GT (2000) Rubber Chem Technol 73(4):647
19. Luginsland HD, Frohlich J, Wehmeier A (2002) Rubber Chem Technol 75:563

20. Clément F, Bokobza L, Monnerie L (2005) Rubber Chem Technol 78:211
21. Payne AR (1960) J Appl Polym Sci 7:127
22. Shim SE, Isayev AI (2004) Rheol Acta 43:127
23. Aranguren MI, Mora E, Macosko CW (1997) J Colloid Interf Sci 195:329
24. Sahakaro K, Beraheng S (2008) J Appl Polym Sci 109:3839
25. Zhu ZY, Thompson T, Wang SQ, von Meerwall ED, Halasa A (2005) Macromolecules 38:8816
26. Daoud WA, Xin JH, Tao XM (2004) J Am Ceram Soc 87:1782
27. Yang SY, Chen S, Tian Y, Feng C, Chen L (2008) Chem Mater 20:1233
28. Chen S, Hu CH, Chen L, Xu NP (2007) Chem Commun 1919
29. Huang X, Hu CH, Cai XJ, Chen S (2009) Chin J Inorg Chem 25:184
30. Xu W, Raychowdhury S, Jiang DD, Retsos H, Giannelis EP (2008) Small 4:662
31. Wu YP, Zhao QS, Zhao SH, Zhang LQ (2008) J Appl Polym Sci 108:112
32. Leblanc JL (2002) Prog Polym Sci 27:627
33. Mélé P, Albérola ND (1996) Polym Compos 17:751